CGMS

CGMS-36, NOAA-WP-17
Prepared by M. Goldberg
Agenda Item: II/3
Discussed in WG II

# Climate Data Anomalies and Trends: NOAA Report on Climate Product Research Development

In response to CGMS Action 35.20 (NOAA/NESDIS to include information on global and regional anomalies in their products as well)

NOAA WP-17 reports on information on global and regional anomalies and trends for a number of experimental climate products at NOAA/NESDIS.

# Anomalies and Trends in HIRS Outgoing Longwave Radiation Climate Data Record

**Hai-Tien Lee (CICS/ESSIC-NOAA) Aug. 25, 2008**

The multi-spectral method developed by Ellingson et al. (1989) can accurately estimate the outgoing longwave radiation (OLR) at the top of the atmosphere directly with the narrow-band radiance observations. The NESDIS implemented this algorithm and has been generating OLR product operationally using High-resolution Infrared Radiation Sounder (HIRS) observations since 1998.

The complete retrospective HIRS OLR retrievals were performed with the reprocessing of the entire collection of HIRS Level-1b data sets dated back to late 1978. Methodologies were developed to ensure continuity and homogeneity of the HIRS OLR time series. These works led to the first release (denoted Edition 2) of the HIRS OLR climate data record spanning from 1979 to 2003 (Lee et al., 2007). The preliminary analyses of anomalies and trends discussed here are based on this data set.

The HIRS monthly mean OLR time series was shown to have excellent quality compared to the broadband instruments observations from the Earth Radiation Budget Experiment (ERBE) and the Clouds and the Earth's Radiant Energy System (CERES). Most impressively, the HIRS OLR shows a comparable stability as in the ERBS non-scanner OLR measurements, about 0.3 $Wm^{-2}$ per decade. Note that the ERBS wide-field-of-view (WFOV) non-scanner is by so far considered the most stable earth radiation budget instrument. The mean differences of HIRS and the broadband OLR products are within the limit of the absolute radiometry accuracy, about 2% in ERBE and 1% in CERES. The rms differences of HIRS and CERES monthly mean OLR products are about 5 $Wm^{-2}$.

**Tropical**

Figure 1 shows the tropical (20°S-20°N) mean OLR time series determined by HIRS and the broadband instruments including ERBE scanner/non-scanner CERES scanner. It shows that the HIRS OLR reproduced the tropical OLR variability in high accuracy compared to the broadband products.

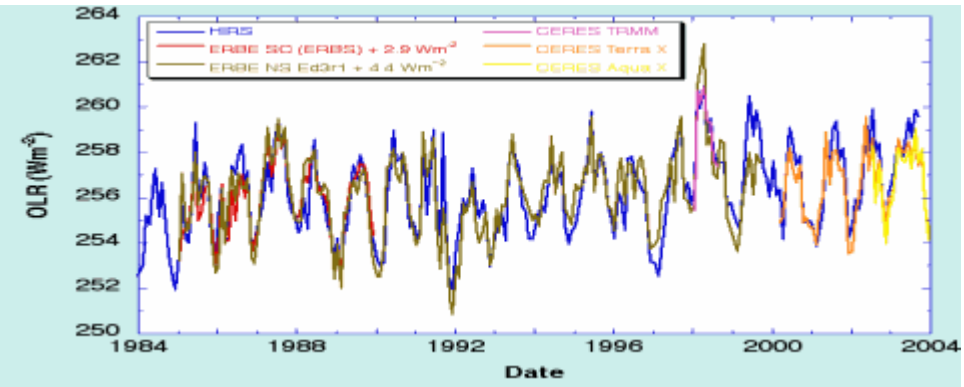


***Fig. 1. Tropical (20°S-20°N) mean OLR time series determined by HIRS and the broadband instruments including ERBE scanner/non-scanner CERES scanner. The ERBE scanner and non-scanner results were adjusted to compensate the estimated biases.***

Wielicki et al. (2002) on Science reported a significant tropical OLR decadal change of +3.1 $Wm^{-2}$ (average of 1994-97 minus 1985-89) based on ERBS Ed. 2 data set. This was not supported by HIRS OLR data at the time. The ERBS Ed. 2 data was later found to have errors resulted from a software bug that neglected satellite altitude correction, and from

daytime shortwave under-estimation that led to the longwave overestimation. The revised data set (ERBS Ed. 3 Rev.1) now showed a +0.6 $Wm^{-2}$ decadal change that is then more agreeable to the HIRS's result of +0.2 $Wm^{-2}$. The consensus is that there is no significant decadal change in OLR in the tropics between 1980's and 90's. However, ERBS data suggested a net heating to the earth-atmosphere system of about 1.5 $Wm^{-2}$.

**Global**

Figure 2 shows the time series of the global mean OLR determined by the HIRS OLR data set, as well by ERBE and CERES Scanner observations, and ISCCP FD data set. The linear trend of HIRS global mean OLR in 1979 to 2002 is 1.34±0.21 $Wm^{-2}$ per decade.

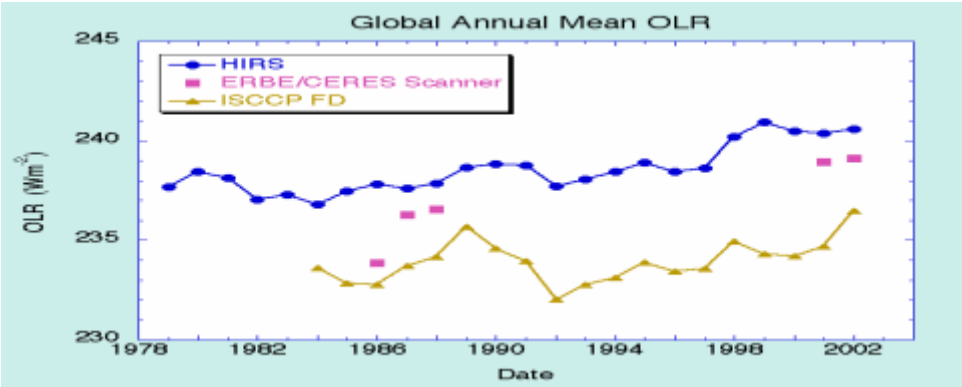


***Fig. 2. Global mean OLR time series determined by HIRS, the broadband instruments including ERBE and CERES scanner, and ISCCP FD data sets.***

The surface temperature trends of for the same period were determined from three data sources: CRU, GISS and NCDC that show very similar results.

| | CRU Jones | GISS Hansen | NCDC |
|---|---|---|---|
| **Surface Temperature trend** | 0.169±0.03 °C per decade | 0.154±0.03 °C per decade | 0.164±0.03 °C per decade |

Although inter-annual variations of OLR and surface temperature are relatively closely followed one to another (figure at right), the magnitude of the surface temperature trend alone is insufficient to explain the OLR trend when one assumes a typical 1.7 $Wm^{-2}$/°K climate sensitivity.

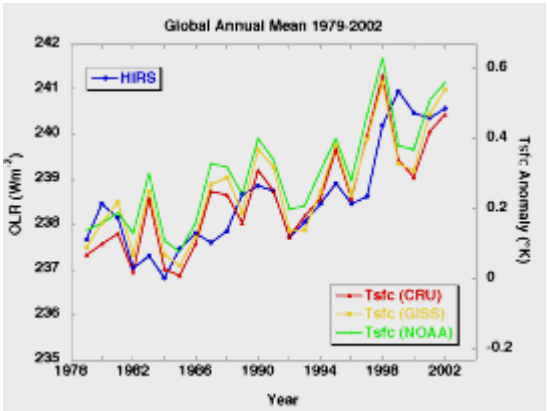

We estimated the global cloud cover trend required to satisfy the given OLR and temperature trend conditions using parameterizations derived in past studies.

Following Budyko (1969):

$$OLR = 226 + 2.26\,T_s \quad (48 \quad 1.62T_s)A_c$$

Given 1979-2002 linear trends of OLR 1.34 $Wm^{-2}$/decade and $T_s$ 0.17°/decade, we estimated the linear trend in global cloud cover would be about -1.5% per decade at a mean cloud cover fraction of 0.6 and a mean surface temperature of 15°C.

Following Cess (1976):

$$OLR = 257 + 1.57\,T_s \quad 91A_c$$

Given the same trends in OLR and Ts, we estimated the linear trend in global cloud cover would be about -1.2% per decade.

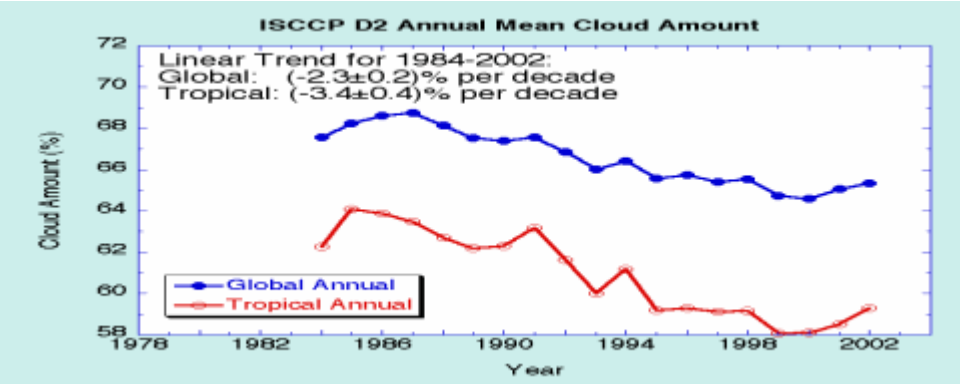


***Fig. 3. Global and tropical mean cloud cover time series derived from ISCCP D2 data set that shows a linear trend of -2.3% per decade in global cloud cover for 1984-2002 period.***

The ISCCP D2 data seems to support this analysis with its linear global cloud cover trend of (-2.3±0.2)% per decade for the period 1984-2002. For the same period, the OLR and surface temperature linear trends become 1.88 $Wm^{-2}$/decade and 0.21°C/decade, respectively. Correspondingly, a cloud cover change was estimated to be about -1.7 to -2.2% per decade and this is within the uncertainty of that observed by ISCCP. This analysis provided very good evidence showing coherent variability among OLR, surface temperature, and the cloud cover that indirectly proved the validity of the long-term variability in these data sets.

**References**

Ellingson, R. G., D. J. Yanuk, H.-T. Lee and A. Gruber, 1989: A technique for estimating outgoing longwave radiation from HIRS radiance observations. *J. Atmos. Ocean. Tech.*, **6**, 706-711.

Lee, H.-T., A. Gruber, R. G. Ellingson and I. Laszlo, 2007: Development of the HIRS Outgoing Longwave Radiation climate data set. *J. Atmos. Ocean. Tech.,* **24**, 2029–2047.

HIRS OLR Data Access: http://cics.umd.edu/~lee/HIRS_OLR.html

## B. SBUV/2 Ozone Record: Updated Accomplishments (Larry Flynn)

The NOAA SBUV/2 instruments are continuing the atmospheric ozone record. The Version 8 total ozone and profile algorithms developed for TOMS and SBUV/2 have replaced the older Version 6 algorithms in both the reprocessing and operational systems. The operational SBUV/2 data from NOAA-16 and NOAA-17 were used to monitor the Antarctic Ozone Hole and appeared in the NOAA Southern Hemisphere Winter Summary (1). Sample plots from the latter are shown on the next pages. The 2008 Ozone hole will be monitored at NOAA with information from NOAA-16, -17 and -18 SBUV/2s, MetOp-A GOME-2, and EOS Aura OMI.

Action Completion: Long-term data records from the SBUV(/2) series (1979-2003) were provided on a DVD in 2004 and were used in the latest WMO 2006 Ozone Assessment. An extension of that record is now available via anonymous ftp at ftp://ftp.orbit.nesdis.noaa.gov/pub/smcd/spb/ozone/dvd_v8_extended/
The extension contains the reprocessed SBUV/2 ozone profile and total ozone data records for NOAA-16 (2004-2007) and NOAA-17 (2003-2007) with retrospective calibration and characterization, thus adding four years to the 25-year SBUV(/2) CDR.

On-going Action: We are still studying the characterization for NOAA-14 (1996-2003) and NOAA-18 (2005-present) and plan to add them to the CDR when progress merits their inclusion. The NOAA-16 SBUV/2, NOAA-17 SBUV/2, and NOAA-18 SBUV/2 are continuing to make measurements. NOAA also plans to launch an SBUV/2 on NOAA-19 early next year. All four SBUV/2s will be reprocessed to continue the long-term ozone monitoring program.

Impact: We have extended the 25-year SBUV/2 CDRs (1979-2003) by four years. These four years cover a period of interest for ozone recovery characterization. The division of the attribution of this neonascent recovery between dynamics and chemistry is open to debate. The extended CDR is expected to be used by the 2010 Ozone assessment panel. The first instalment of this extension consists of the NOAA-16 and NOAA-17 components, and has been released at the NESDIS/STAR anonymous ftp site. We will work to add the NOAA-14 SBUV/2 data to fill in a gap in the Ozone CDR in the late 1990s and continue the record over the coming years.

We are working with the OMI and GOME-2 teams to ensure that both operational and long-term monitoring make the best and consistent use of ozone products from current sensors. We are using Near-Real-Time OMI products and processing GOME-2 data operationally with the Version 8 total ozone algorithm. We are working with the NASA Measures Program to create Version 8 ozone profile CDRs from the OMI record. We are also collaborating with the Chinese as they work on producing ozone estimates from the recently launched SBUS and TOU instruments on FY-3. Ozone monitoring at NOAA will continue with one more SBUV/2 on NOAA-19 (NOAA-N'); followed by the OMPS on NPP and NPOESS.

(1) http://www.cpc.ncep.noaa.gov/products/stratosphere/winter_bulletins/sh_07/

| | |
|---|---|
| TOMS | Total Ozone Mapping Spectrometer |
| SBUV | Solar Backscatter Ultraviolet instrument |
| OMI | Ozone Monitoring Instrument |
| GOME | Global Ozone Monitoring Experiment |
| SBUS | Solar Backscatter Ultraviolet Sounder |
| TOU | Total Ozone Unit |
| OMPS | Ozone Mapping and Profiler Suite |

Figures 4 and 5 in this document are figures 5 and 14 in the Southern Hemisphere Winter Bulletin at http://www.cpc.ncep.noaa.gov/products/stratosphere/winter_bulletins/sh_07/

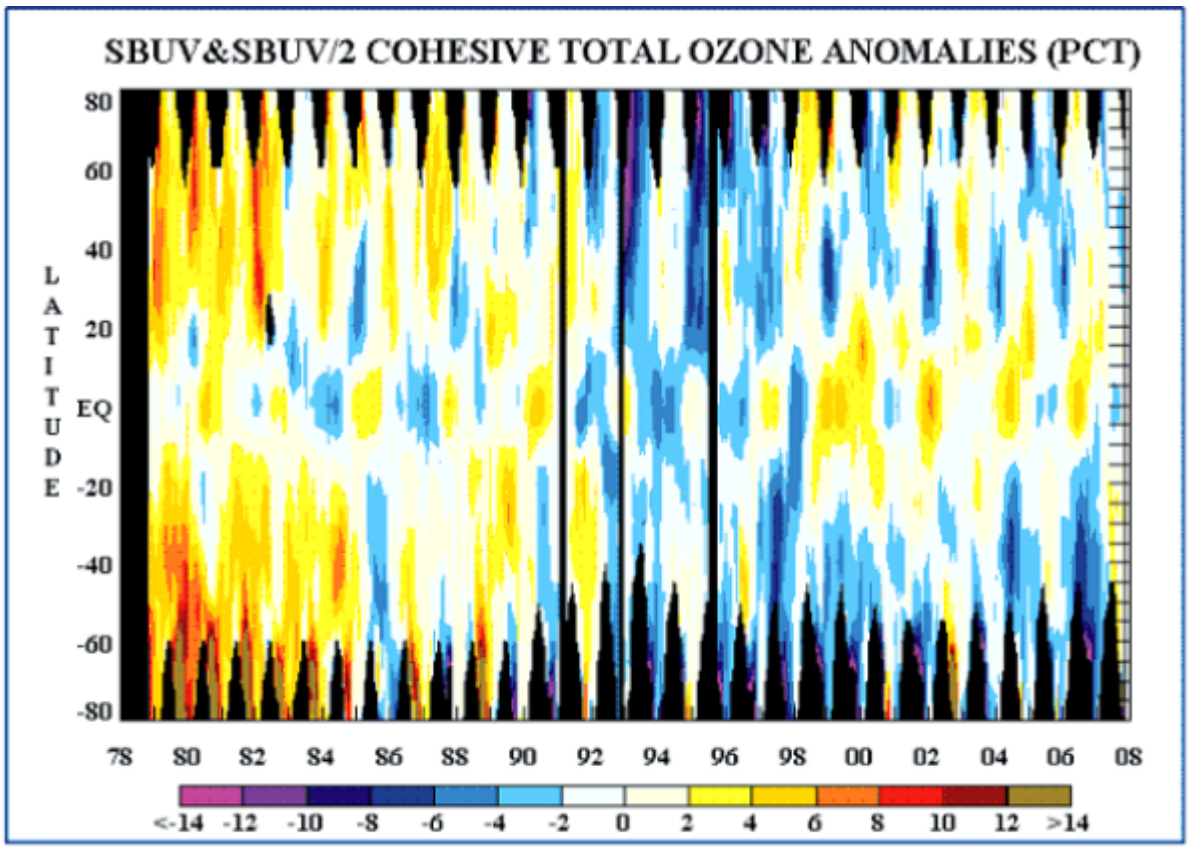


**Figure 4**. Time series of monthly average anomalies (percent) of zonal mean total ozone derived from Nimbus-7 SBUV (11/1979 - 12/1988), NOAA-11 SBUV/2 (01/1989-12/1993), NOAA-9 SBUV/2 (01/1994 - 12/1995), NOAA-14 (01/1996 - 12/1998), NOAA-11 (01/1999 - 12/2000), NOAA-16 (01/2001 - 12/2005), and NOAA-17 (01/2006-present). Black areas indicate insufficient sunlight to make measurements.

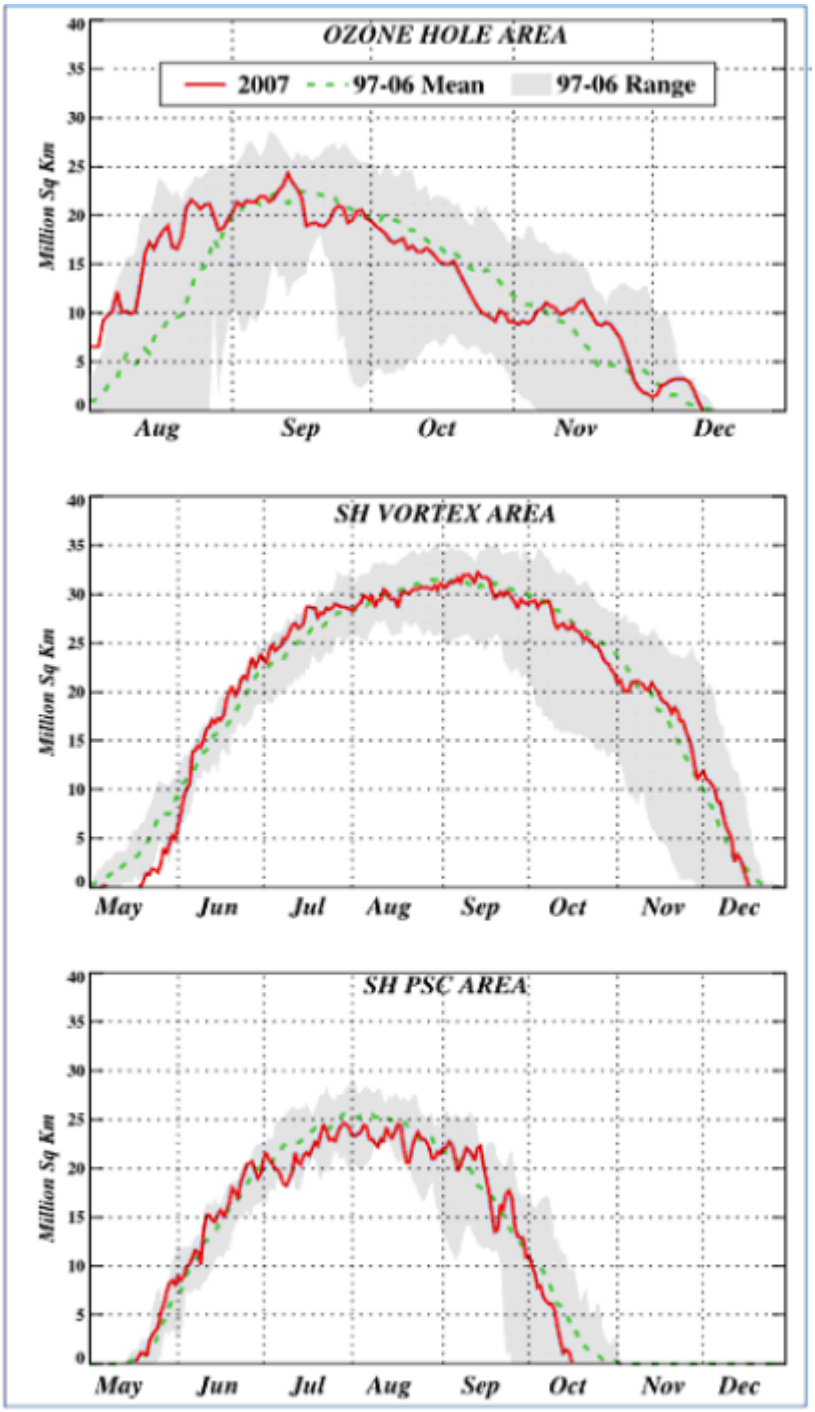


**Figure 5.** Time series of area of the 2007 ozone hole (total ozone < 220 DU), size of SH polar vortex (defined as -32 PVU contour enclosed area at 450K isentropic surface), and size of area of temperature < -78 C (also on the 450K isentropic surface). The shaded region illustrates the range of area sizes over the past ten years (1997-2006). The dashed line is the daily mean area for the past ten years.

**The SBUV/2 was featured at the Quadrennial Ozone Symposium in Tromso Norway**

Selected presentations related to SBUV/2

**New developments in observational techniques**

- M. DeLand: Inflight Calibration Analysis for SBUV/2 Ozone Data
- S. Taylor: Local Time Effects on SBUV Ozone Measurements and Analysis

**Observations - total ozone, vertical distribution, analysis and evaluation**

- L. Flynn: Measurements and Products from NOAA SBUV/2 and OMPS Instruments
- V. Fioletov: The performance of the ground-based total ozone network assessed using satellite data
- V. Fioletov: Estimating ozone variability and instrument uncertainties from SBUV(/2), ozonesonde, Umkehr and SAGE II measurements
- S. Frith: 29 Years of Ozone Profile Data from SBUV Instruments: A Continuous Coherent Data Set
- R. McPeters: SAUNA Ozone Profile Comparison: SBUV/2 and MLS versus sondes and lidar

**Ozone depletion in a historical perspective**

- V. Fioletov: Global and zonal total ozone variations: 1964-2007

**Ozone recovery**

- S.K. Yang: Statistical Examination of the Trend and Change in Trend of Total Ozone at Various Latitudes
- R. Stolarski: Using the SBUV Ozone Profile Data Set to Search for Signs of Ozone Recovery
- J. Krzyscin: Regression model for data with time-varying trend component: Examination of SBUV V8 merged profile ozone for the period 1970-2007

**Climate ozone interaction**

- S. Zhou: The influence of global ozone recovery on the lower stratospheric temperature
- S. Lloyd: Trends in Southern Hemisphere Albedo using a 27-yr Composite TOMS/SBUV(/2)/OMI Dataset of UV Lambertian Equivalent Reflectivity (LER)

## C. Anomalies and Trends in Sea Surface Temperatures and associated clear-sky radiances over oceans (Alexander Ignatov, Prasanjit Dash, XingMing Liang, Yury Kihai, John Sapper)

In the 1970s, NOAA/NESDIS pioneered Sea Surface Temperature (SST) operational products from AVHRR. Associated clear-sky Brightness Temperatures (BT) in AVHRR thermal bands centered at 3.7, 11, and 12 μm have been also used in the Numerical Weather Prediction (NWP) model applications. Heritage SST production has been performed within the Main Unit Task (MUT) system.

A web-based system has been established to calculate SST anomalies with respect to multiple global reference SST fields including Reynolds SST (NESDIS/NCDC), OSTIA (UKMO), ODYSSEA (French Met Service), etc. Global anomalies are posted at http://www.star.nesdis.noaa.gov/sod/sst/gqt/ in near-real time. The objective is monitoring SST products for stability and cross-platform consistency.

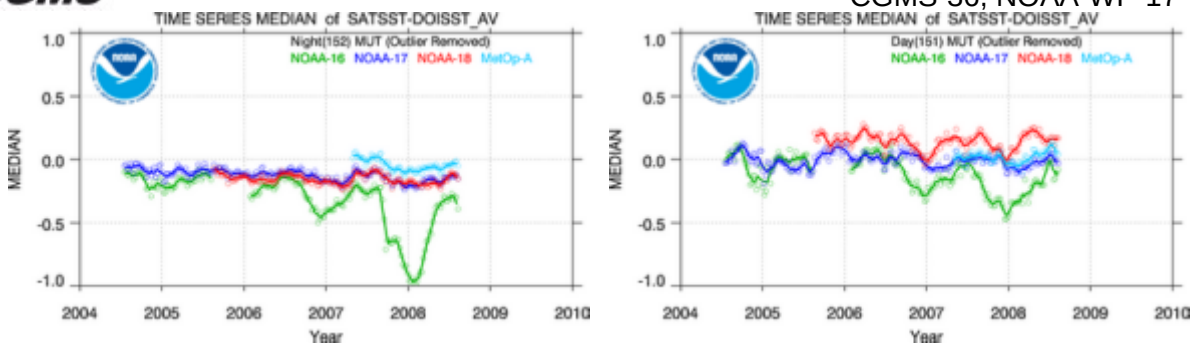


***Fig.6. Global median of "retrieved minus Reynolds" SST anomaly from 4 AVHRR instruments onboard NOAA-16, -17, -18, and MetOp-A platforms. Left: nighttime; right: daytime. Warm bias in MetOp-A nighttime SST is likely due to SST bias error. NOAA-16 anomalies are likely due to malfunction of the AVHRR sensor. During daytime, morning NOAA-17 and MetOp-A are consistent, whereas the afternoon NOAA-18 shows diurnal warming.***

A new AVHRR Clear-Sky Processor for Oceans (ACSPO) has been recently developed to replace the MUT system. Similar to MUT, it generates three products over oceans: clear-sky BTs, SST and Aerosol. Community Radiative Transfer Model (CRTM) is incorporated in ACSPO and used in conjunction with global forecast fields to calculate the model clear-sky BTs. Model minus observation (M-O) bias is subsequently calculated and trended over time at http://www.star.nesdis.noaa.gov/sod/sst/micros/ for stability and cross-platform consistency. An example is shown in Figure 7.

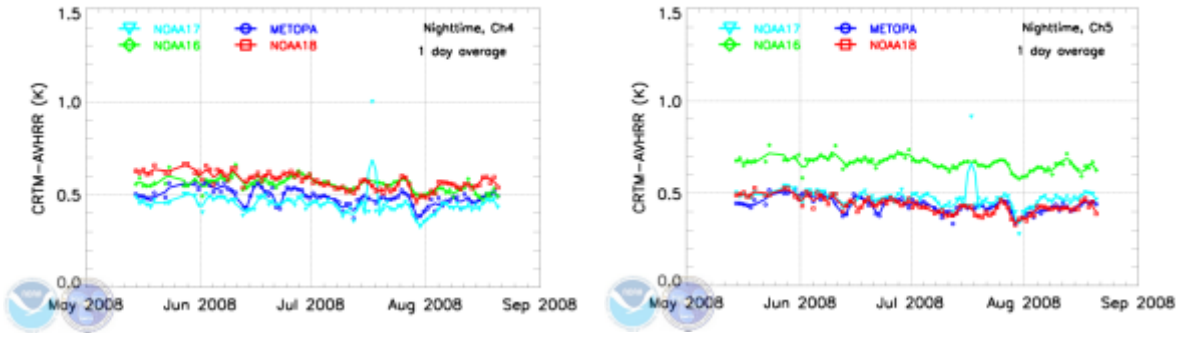


***Fig.7. Global nighttime 'M-O' bias for 4 AVHRR instruments onboard NOAA-16, -17, -18, and MetOp-A platforms. Left: Ch4; right: Ch5. Model is warmer than observations, because aerosol effects are not included in CRTM and bulk SST is used as input. Also, AVHRR BTs may be subject to residual cloud. In Ch4, M-O biases are largely consistent across different platforms, whereas in Ch5 NOAA-16 is out of family, likely to sensor problems.***

ACSPO improvements are underway and stewardship system is being set up which allows generating high-quality climate data records (CDRs), by multiple passes through the historical AVHRR data. The ACSPO development strives to preserve consistency between current and future sensors onboard POES and GOES platforms. Work is also underway to generate AVHRR-like clear-sky BTs, SST, Aerosol products from NPOESS/VIIRS and GOES-R/ABI. MSG/SEVIRI is used as GOES-R/ABI proxy. The emphasis is on synergy between Clear-Sky Radiances, assimilated by the NWP models, and SST and Aerosol, used in oceanographic, ecological, atmospheric and climate research. ACSPO extensively uses accurate radiative transfer models in conjunction with global forecast fields, to improve cloud screening, quality control, and inversion accuracy.

***Significance***: AVHRR time series span 25+ years and are well suited for generating climate data records of CSR, SST and Aerosols, consistent with newer sensors explored. The project is linked to CEOS and GOOS objectives. Long-term stability and cross-platform consistency of SST and clear-sky brightness temperature products, which emphasizes their anomalies with respect to a known reference, is critically important for the quality of climate data records.

***References***:

Ignatov, A., J. Sapper, et al. 2005: Global diagnostics of operational AVHRR SST and aerosol retrievals from NOAA-16 and NOAA-17. *Proc. SPIE*, **5658**, 206-215.

Ignatov, A., J. Sapper, et al, 2004: Global operational SST and Aerosol products from AVHRR over ocean: Current status, diagnostics, and potential enhancements. 13th AMS Conf. on Satellite Meteorology and Oceanography, 20-23 Sep 2004, Norfolk, VA, 12pp.

Dash, P., A. Ignatov, Y. Kihai, J. Sapper, 2008: Long-term stability and cross-platform consistency of AVHRR SST. *Remote Sensing Environment*, in prep.

Liang, XM., A. Ignatov, and Y. Kihai, 2008: Implementation of the Community Radiative Transfer Model (CRTM) in the AVHRR Clear-Sky Processor for Oceans (ACSPO) and Validation against Nighttime Radiances. *J. Geophys. Res*, submitted.

***Websites***: http://www.star.nesdis.noaa.gov/sod/sst/gqt/ &
http://www.star.nesdis.noaa.gov/sod/sst/micros/

***Collaboration***: NCDC, NODC, NAVO, U. Miami, GHRSST.

## D. Analysis of Trends in Aerosol Optical Depth in the AVHRR Pathfinder Atmospheres Extended (PATMOS-x) data (Istvan Laszlo and Xuepeng Zhao)

A nearly 25-year aerosol record was constructed from radiances in the Advanced Very High Resolution Radiometer (AVHRR) Pathfinder Atmosphere extended (PATMOS-x) data set. The PATMOS-x radiances are the result of improvements in AVHRR calibration and geolocation. The radiances used for aerosol retrieval are also benefited from improved cloud information in the PATMOS-x processing. Daily orbital clear-sky PATMOS-x radiances, mapped into $0.5^o$x$0.5^o$ grids, were used to retrieve aerosol optical depth (AOD) at 0.63 and 0.83μm over ocean using a revised independent two-channel aerosol retrieval algorithm. The retrieved AOD values were further averaged to $1^o$x$1^o$ grids, and the latter were used to calculate monthly, seasonal, and annual mean values. An analysis of the globally and monthly averaged 0.63-μm AOD in this data set yielded a small, but statistically significant, linear trend of -0.01/decade, indicating a small reduction of aerosol in the atmosphere. The trend is even more evident for globally and annually averaged AOD and its magnitude can be up to -0.03/decade. This trend agrees in sign with, but about twice as large as the trend found from the independently derived data from the Global Aerosol Climatology Project. Decrease in northern hemisphere AOD (-0.03 per decade) is larger than that in the southern hemisphere (-0.02 per decade). Regionally, changes in aerosol amounts vary in magnitude and sign. Areas affected by emissions from developed western countries show a decrease, while those affected by emissions from the fast developing Asian countries show an increase in aerosol amount. Long-term changes in regional AOD also vary with seasons. In general, negative trends are observed for seasonally averaged AOD in the regions influenced by the emissions from industrialized countries and the magnitude can be up to -0.10/decade. Increases are observed in the regions influenced by emissions from the fast developing countries and the magnitude can be up to +0.04/decade. For regions heavily influenced by desert dust from the Sahara, a negative trend with a maximum magnitude of -0.03/decade is detected. However, over the regions influenced by smoke from biomass burning, positive tendencies with a maximum magnitude of +0.04/decade are observed.

Recommendations

The PATMOS-X based aerosol data set currently is only available by request. It is recommended to host the aerosol data in a publicly assessable location with proper documentation.

Contribute to the GEWEX Aerosol Assessment project.

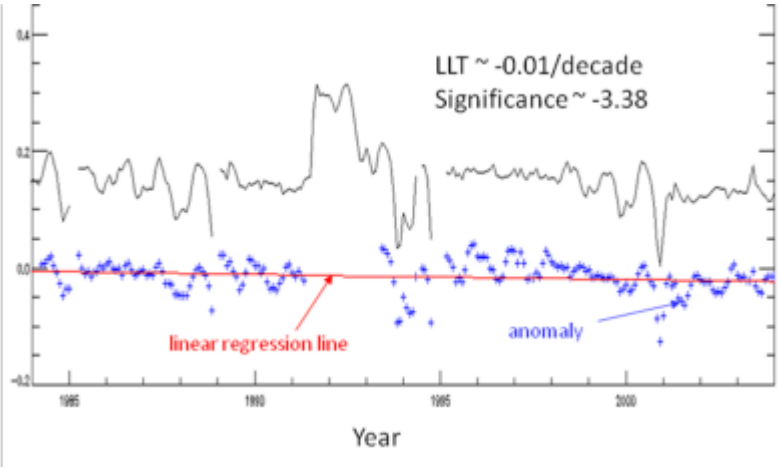


*Figure 8. Time series of monthly averaged AOD (curve) and its anomaly (plus signs) along with the linear regression of the anomaly (straight line). The linear long-term trend (LLT) and its significance (ratio of LLT to standard deviation) are also given.*

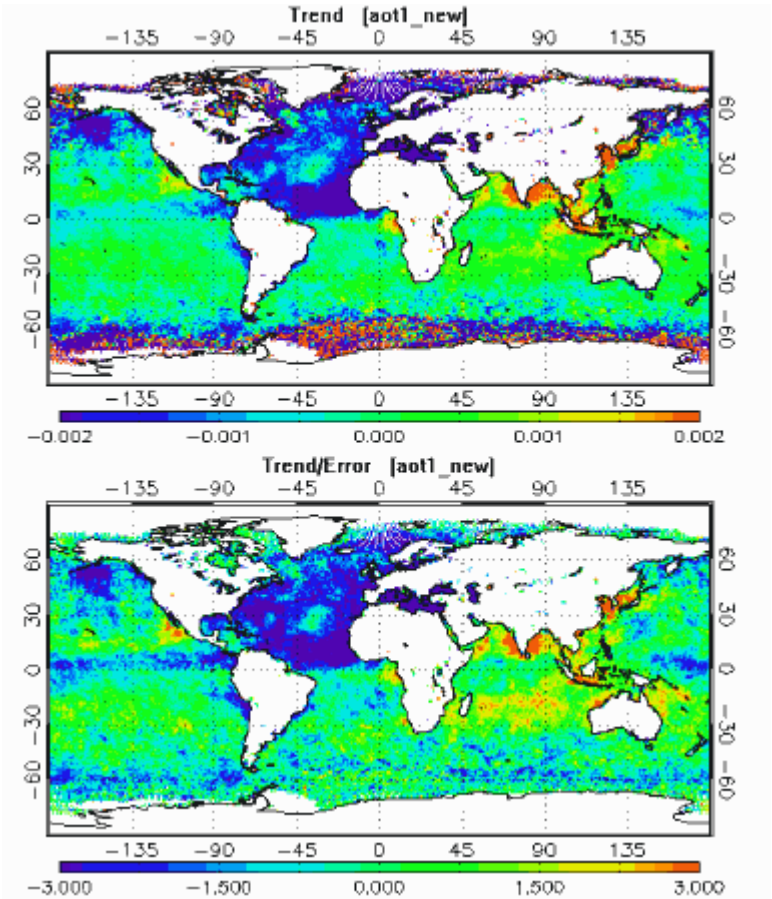


*Figure 9. Maps of linear long-term trend (top) and significance of trend (bottom) derived from monthly average AOD. Significant decrease in AOD is observed over the northern Atlantic Ocean, the Mediterranean, along the coast of Europe and the west east coast of North America. Positive trends are shown around the south coast of Asia, especially India and China.*

## E. Status of SSM/I Climate Data Sets at NESDIS

(Updated 20 August 2008)

Ralph Ferraro and Fuzhong Weng, NOAA/NESDIS/STAR

Satellite measurements from the Defense Meteorological Satellite Program's (DMSP), Special Sensor Microwave/Imager (SSM/I) is the longest time series of satellite microwave imager in existence today, over 21 years in length (starts in July 1987). These observations are being followed with a nearly identical sensor, the Special Sensor Microwave Imager/Sounder (SSMIS), which will continue to operate for at least the next decade. This sensor will ultimately be replaced by the Microwave Imager/Sounder (MIS) on NPOESS, continuing this record of passive microwave measurements well beyond 2020.

Through several years of support from NOAA/Office of Global Programs, the SSM/I data have been used to generate a valuable time series (pentad and monthly, 1.0 and 2.5 degree grid) of hydrological products (including rain, snow, ice, cloud liquid water, and total precipitable water) which are archived at NCDC and are updated on a monthly basis **(http://lwf.ncdc.noaa.gov/oa/satellite/ssmi/ssmiproducts.html).** They contribute significantly towards NOAA's Climate Mission Goal (e.g., NCEP's *Climate Diagnostic Bulletin)* and international programs (e.g., the Global Precipitation Climatology Program – GPCP).

Figure 10 shows the global mean annual rainfall as derived from the SSM/I; the major rainfall and desert regions are clearly indicated. Seasonal to interannual variations of rainfall can clearly be monitored from this time series. For example, Figure 11 shows the rainfall anomalies over the tropical Pacific "Nino 4" region. Note that the strong positive and negative anomalies correspond to warm and cold SST episodes, respectively.

Snow cover is another important parameter that is retrieved from the SSM/I and it complements similar products derived from visible sensors. Advantages of the microwave retrievals are its ability to track snow cover during both and day time, as well as under cloudy conditions. Figure 12 shows the SSM/I derived January and July climatologies of snow cover frequency.

Although the quality of this SSM/I time series is not robust enough for precise trend analysis (see section below), one can try to get a first order approximation of potential trends during the 21-year period. As an example, Figure 13 shows the global oceanic time series in total precipitable water (TPW) based on pentad data. In this analysis, virtually no trend in TPW on a global basis was found.

However, there are several serious flaws that need to be corrected to make these products true Climate Data Records (CDRs), as detailed in the NRC report published in 2004 (Climate Data Records From Environmental Satellites. *National Research Council of the National Academies).* This work must continue over the next several years, however, sustained funding sources have not been identified. Some initial efforts have been undertaken at NESDIS/STAR and NESDIS/NCDC over the past two years to address some of these deficiencies and to move towards CDR's. The list of tasks and their status are as follows:

Obtain and establish a baseline SSM/I TDR data set in a standard format that will be accessible by the scientific community. In particular, the data sets from the first five years of SSM/I operation were provided in several formats. In addition, develop a metadata database that will contain all of the necessary information on the sensor so that the newly developed calibration information can be repeated by the science community. This data will be archived at NCDC. **Status:** Nearly 95% of the SSM/I TDR archive has been "rescued" and has been QC'd. The data has been placed into NetCDF format has been and will be available through NCDC sometime in 2008.

Perform non-linear and inter-sensor calibration of the entire SSM/I and SSMIS time series (seven satellites at present) to remove the biases and correct the diurnal variation from the orbit drifts. Special treatment for the F-16 SSMIS will be required. This will then be

used to regenerate the SSM/I TDR and SDR data sets, which will be archived at NCDC. These will form SSM/I and SSMIS (henceforth referred to as SSM/I/S) FCDRs. **Status:** Corrections have been developed for the majority of the SSM/I sensors, however, no regeneration of the TDR and SDR has occurred due to lack of funding. Preliminary impact studies show significant differences between uncorrected and corrected TDR data (see Figure 14 as an example).

Utilize the full swath FCDR data to generate improved EDRs (the current products are generated by a 1/3 degree daily gridded, 1 K accuracy data set). These will form the initial TCDRs using the legacy algorithms already in place. **Status:** Some sensitivity studies have been conducted to determine the impact of using the less precise data.

Use newly developed algorithms to improve the TCDRs (e.g., rainfall, cloud water, precipitable water, snow cover, sea-ice cover, ocean surface wind speed) , as well as some potential new products such as land surface emissivity (all seven channels) ice water content, soil moisture and surface type. **Status:** An updated precipitation algorithm has been developed and applied to the entire SSM/I time series and is being tested in an optimal interpolation scheme with other passive microwave sensors.

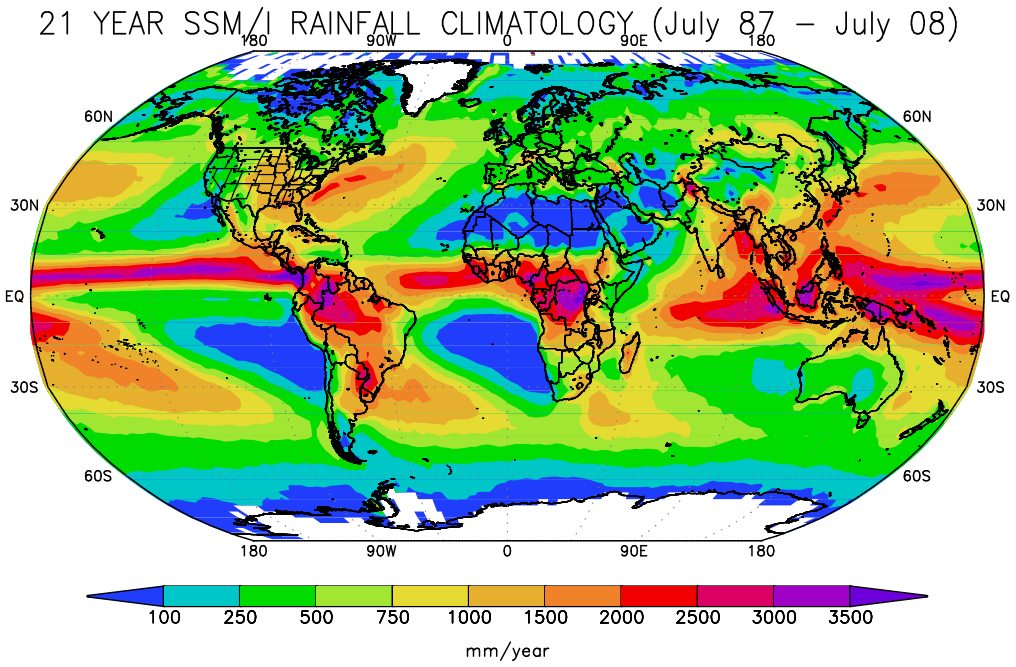


***Figure 10 – Annual mean rainfall (mm/yr) derived from 21 years of SSM/I data.***

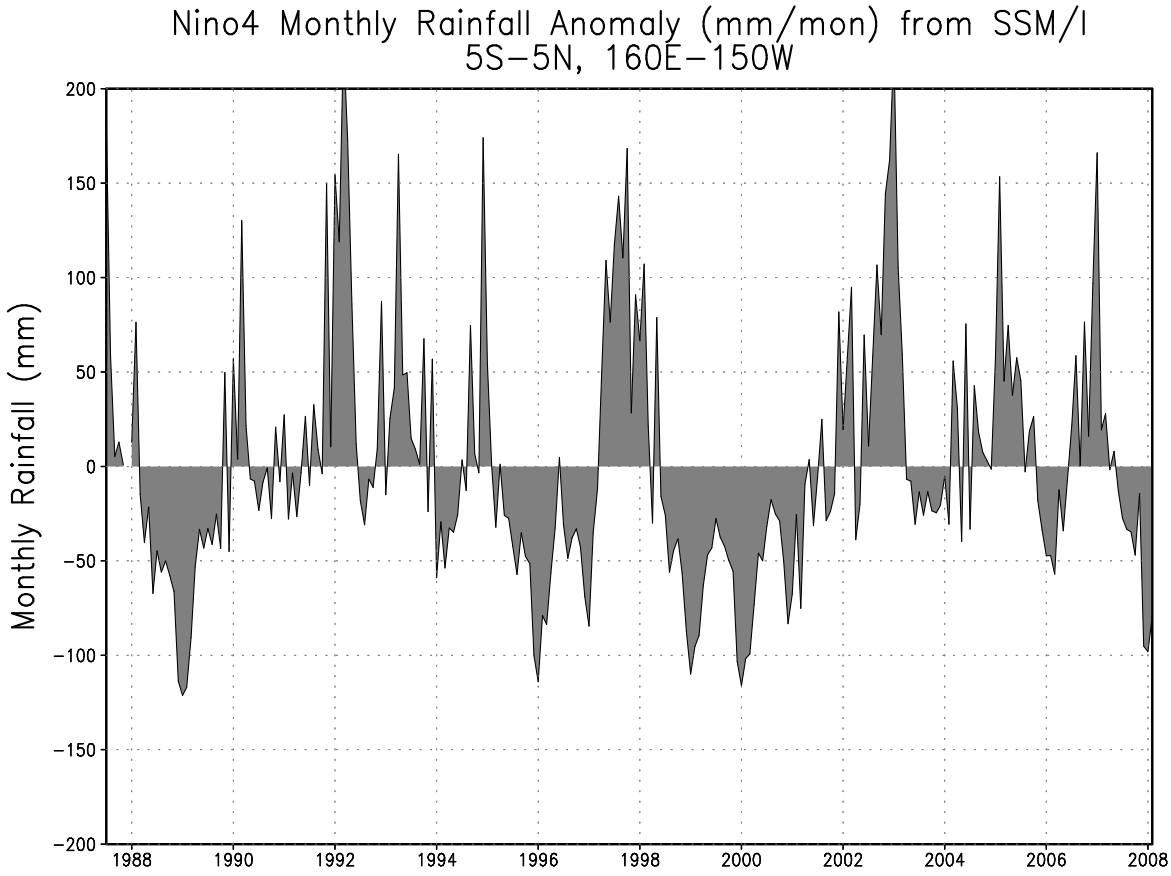


***Figure 11- Monthly rainfall anomaly for the Nino4 region based on the SSM/I climatology. The positive (negative) anomalies correspond to warm (cold) SST events.***

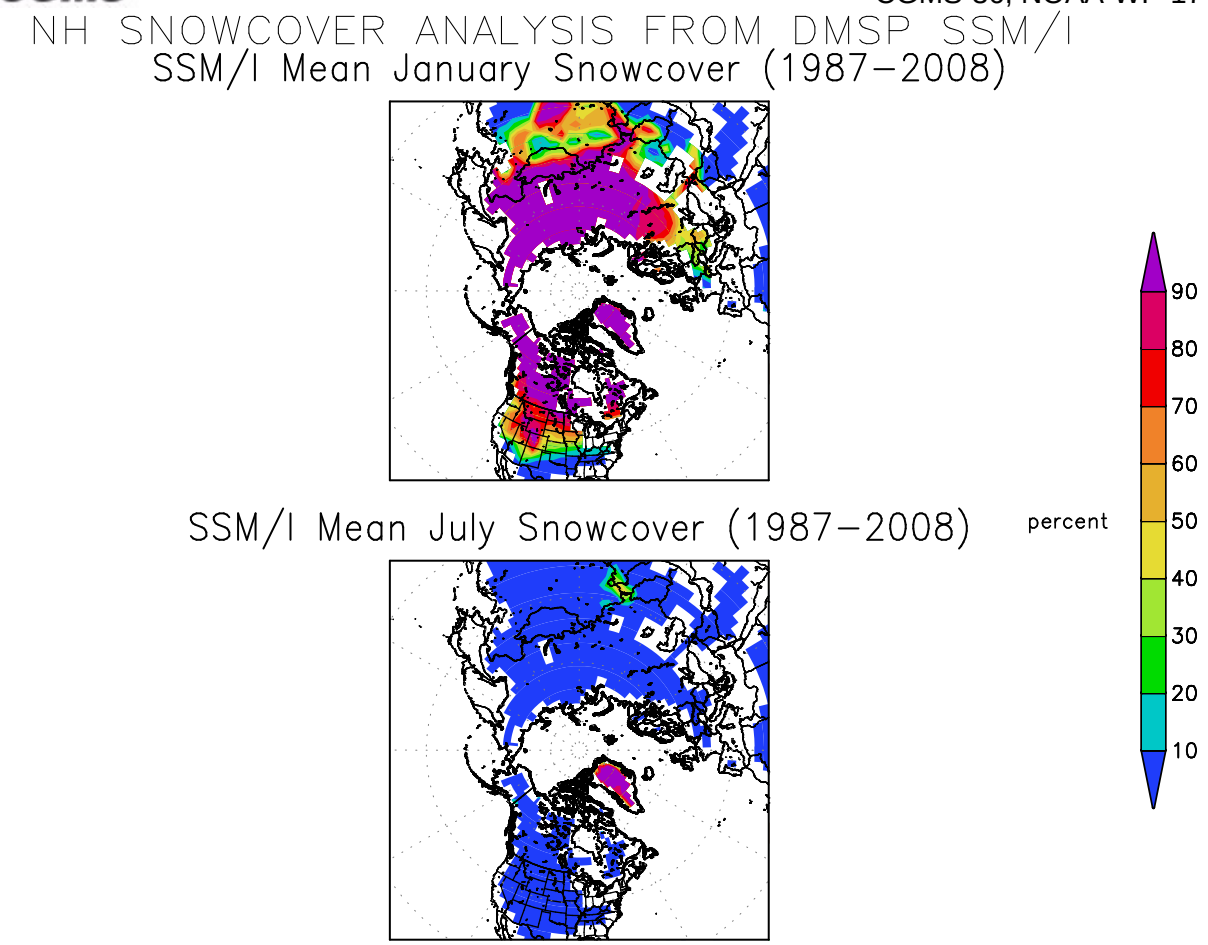


***Figure 12 – Northern Hemisphere snow cover frequency occurrence (percent) for January (top) and July (bottom) based on 21 years of SSM/I data.***

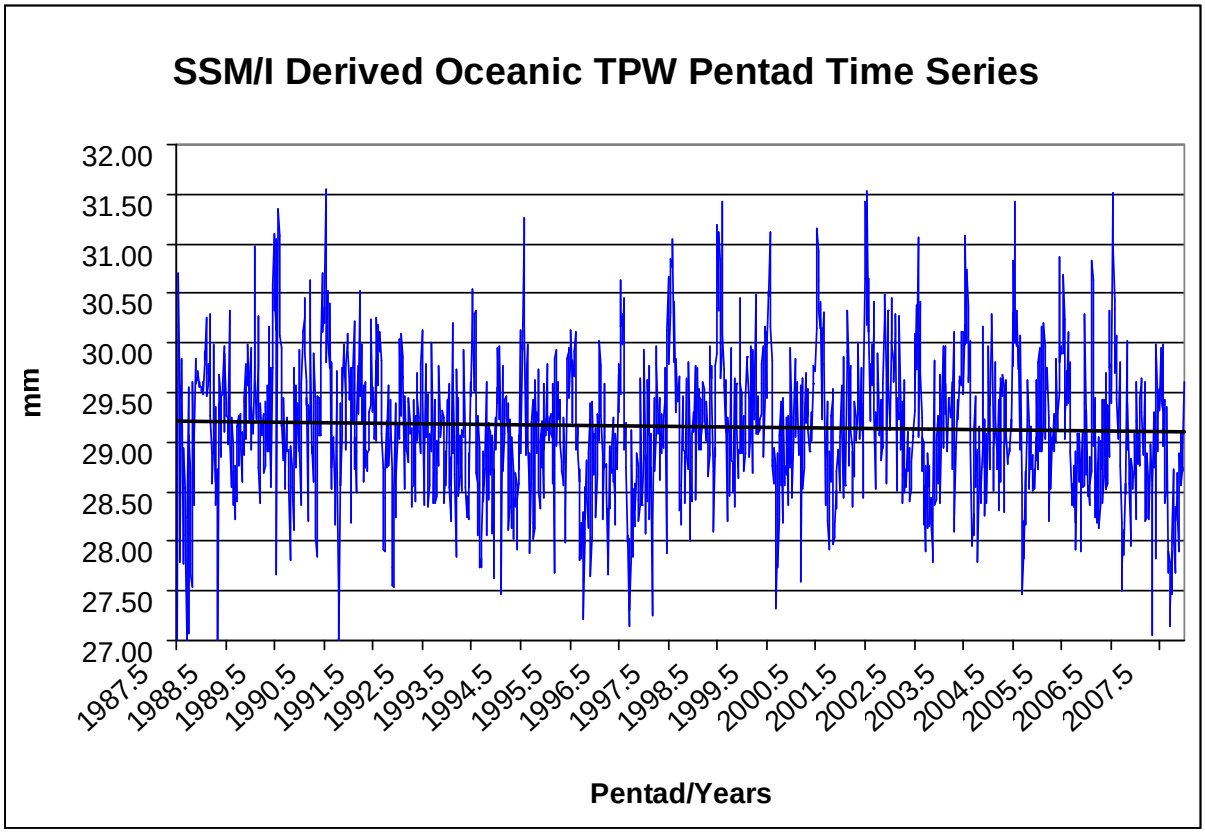


***Figure 13 - SSM/I derived oceanic TPW based on pentad means for the period July 1987 - July 2008. A trend line placed on the time series indicates virtually no trend over the period.***

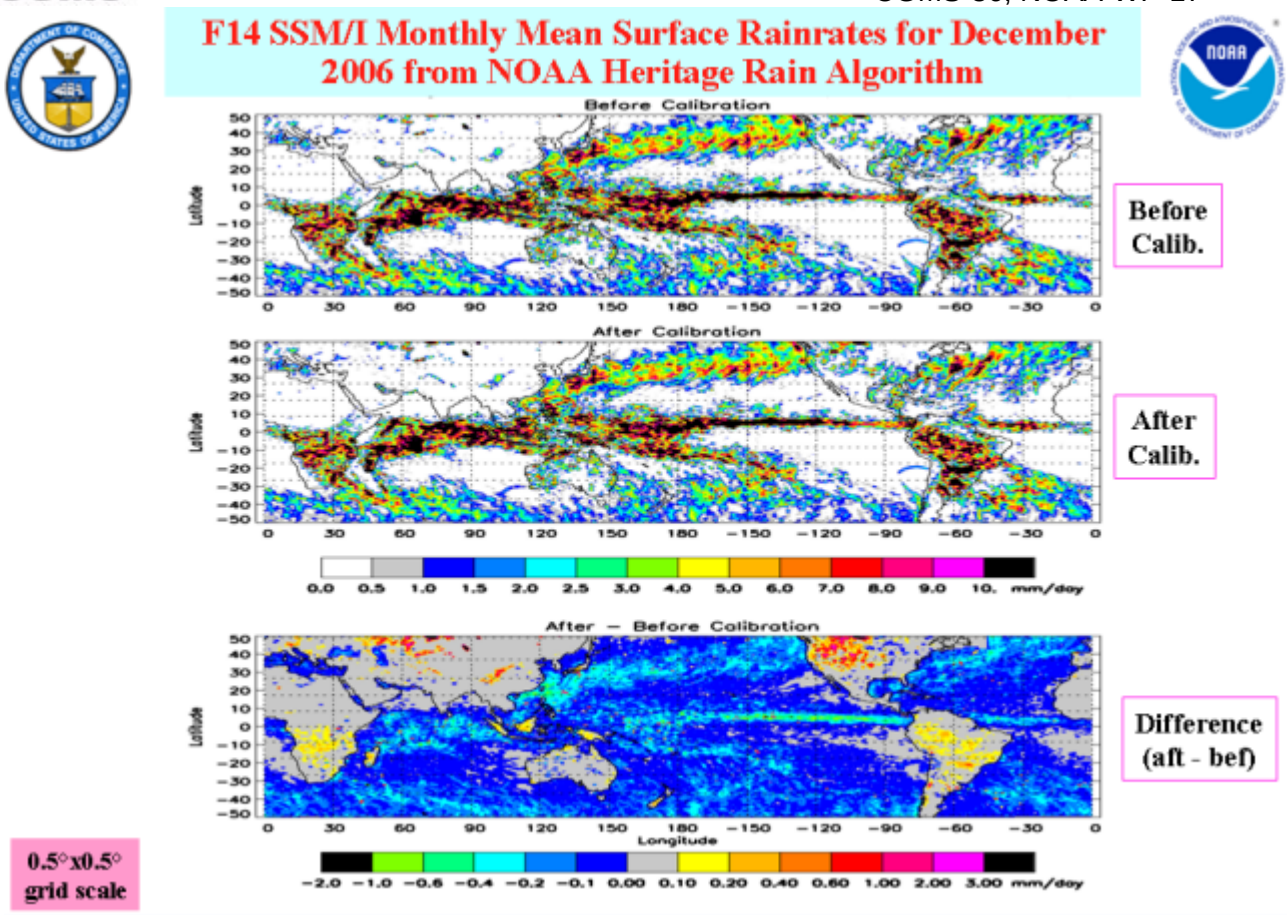


***Figure 14 - SSMI derived monthly precipitation for December 2006 using uncorrected TDR data (top), corrected TDR data (middle) and difference (bottom).***

## F. PATMOS-x: AVHRR Pathfinder Atmospheres Extended (Andrew Heidinger)

The data record from NOAA's Advanced Very High Resolution Radiometer now spans from 1979 to the present and therefore provides almost thirty years of global observations from a nearly consistent satellite instrument. The PATMOS-x project aims to tap into this data-set and provide well-characterized climate data records for cloud, aerosol and surface temperature studies since the beginning of the AVHRR/2 data in 1982. This project was started in 2004 as a climate reprocessing demonstration project within the NOAA/NESDIS Center for Satellite Applications and Research (STAR). PATMOS-x is based on a modified version of the NESDIS operational AVHRR cloud processing system.

To date, the PATMOS-x accomplishments can be summarized as follows.

A contributing data-set to the 2006 and 2007 Cloud and Aerosol Sections of the State of Climate Report of the Bulletin of American Meteorological Society. (Heidinger et al, 2007; Evan and Heidinger, 2007. Evan at el, 2008).
A contributing data-set to the three GEWEX cloud climatology assessment workshops.
PATMOS-x clear radiances used to study long-term trends in aerosol. (Zhao et al, 2008)
Generated first global (land + ocean) multi-year satellite-derived statistics on the frequency of multi-layer cloud. (Heidinger and Pavolonis, 2005)

Generated climatology of the spatial extent of oceanic dust and demonstrated the contribution of the dust variability on the Atlantic SST increases since 1982. (Evan et al, 2008)

Generated a MODIS-based AVHRR reflectance calibration applicable to all satellites in the AVHRR/2 and AVHRR/3 series of sensors (1982-present). (Heidinger et al, 2002)

Over twenty researchers have downloaded the PATMOS-x version-4 data-set.

The following paragraph and associated figure gives an example of the analyses that are being done with PATMOS-x data.

**Impact of Increased Agricultural Biomass Burning on 2007 Cloud Cover in the Amazon Basin**

One advantage of the PATMOS-x data-set is that its data-record extends to the present and new data is added as available. Therefore, PATMOS-x offers the ability to compare current conditions to their variations observed since 1982. We have used this advantage in the analyses shown in the BAMS State of Climate Reports. For example, it has been surmised that increased prices for agricultural products in 2007 spurred an enormous amount of agricultural burning in the Amazon Basin. This generated a record of level aerosol (smoke) over this region which is known to suppress cumulus development via the stabilization of the atmosphere and the reduction in surface heating. PATMOS-x (figure 15) confirmed this behavior and showed statistically significant departures on the order of 5% to 50% in cloudiness.

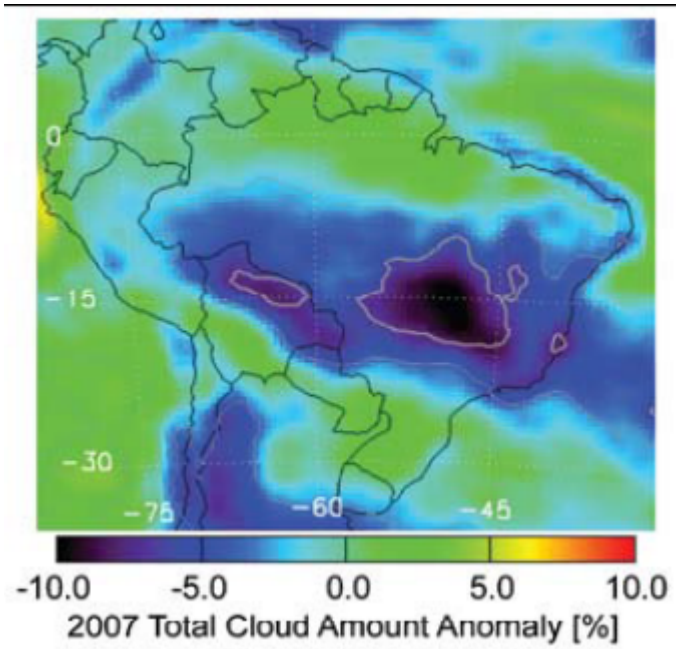


***Figure 15 - Total cloud cover anomaly for 2007 over Brazil. The thin gray contour represents anomalies that are one standard deviation from the climatological mean value, and the thick gray contour represents anomalies that are two standard deviations from the mean state. The likely cause of this anomaly is the dramatic levels of agricultural burning observed in this area for 2007.***

## References

Evan, Amato T.; Heidinger, Andrew K. and Knippertz, Peter. **Analysis of winter dust activity off the coast of West Africa using a new 24-year over-water advanced very high resolution radiometer satellite dust climatology**. Journal of Geophysical Research, Volume 111, 2006, Doi:10.1029/2005JD006336, 2006.

Evan, Amato T.; Heidinger, Andrew K.; Bennartz, Ralf; Bennington, Val; Mahowald, Natalie M.; Corrada-Bravo, Hector; Velden, Christopher S.; Myhre, Gunnar and Kossin, James P.. **Ocean temperature forcing by aerosols across the Atlantic tropical cyclone development region**. Geochemistry, Geophysics, Geosystems, Volume 9, 2008, Doi:10.1029/2007GC001774

Evan, A. Liu, Y., Maddux, B. and Heidinger, A. K., 2008: **Clouds, in State of the climate in 2007.** Levinson, D.H., and J.H. Lawrimore eds., Bulletin of the American Meteorological Society, Volume 89, S107-S109.

Heidinger, Andrew K.; Cao, Changyong and Sullivan, Jerry T. **Using Moderate Resolution Imaging Spectrometer (MODIS) to calibrate advanced very high resolution radiometer reflectance channels**. Journal of Geophysical Research, Volume 107, 2002

Heidinger, Andrew K. and Pavolonis, Michael J.. **Global daytime distribution of overlapping cirrus cloud from NOAA's Advanced Very High Resolution Radiometer**. Journal of Climate, Volume 18, Issue 22, 2005, pp.4772-4784.

Heidinger, A.; Evan, A. and Baum, B.. **State of the climate in 2006. Global climate: Cloudiness**. Bulletin of the American Meteorological Society, Volume 88, Issue 6, 2007, S17-S18.

Zhao, Tom X.-P.; Laszlo, Istvan; Guo, Wei; Heidinger, Andrew; Cao, Changyong; Jelenak, Aleksander; Tarpley, Dan and Sullivan, Jerry. **Study of long-term trend in aerosol optical thickness observed from operational AVHRR satellite instrument**. Journal of Geophysical Research, Volume 113, 2008, Doi:10.1029/2007JD009061, 2008

## G. MSU Temperature Trend Pattern (Cheng-Zhi Zou)

Using the technique of *simultaneous nadir overpasses*, StAR produced a new set of data of deep layer atmospheric temperature from Microwave Sounding Unit (MSU) that are well-intercalibrated for climate research. The new dataset has removed the biases of the MSU instrument going from one satellite to another wherever satellite observations overlap, thus yielding accurate climate trend analysis. The dataset includes three products: deep-layer temperature for the mid-troposphere (MSU channel 2), tropopause (MSU channel 3), and lower stratosphere (MSU channel 4). Figure 16 shows the global ocean mean temperature anomaly time series of the three channels and their spatial trend patterns. Global ocean mean temperature trends for the mid-troposphere, tropopause, and lower-stratosphere during 1987-2006 are respectively 0.20 0.07, 0.065 0.07, and -0.33 0.26 K/Decade. For the mid-troposphere and tropopause, this warming trend comes mainly from the last tend years. In the regional scales, temperature trend values over the tropical and mid-latitudes are generally close to the global means for all three channels. Over the Tropical region, the mid-troposphere ($T_2$) has a warming trend about 0.2~0.3 K/decade. This warming trend gradually increases northward, but decreases southward. The tropopause ($T_3$) is warming at a rate less than the mid-troposphere over the tropics and mid-latitudes for the same period (~ 0.1 K/Decade), while the lower stratosphere ($T_4$) shows a large cooling trend (~ -0.5 K/decade) to compensate the warming trend in the troposphere. Over the Arctic Ocean, a significant warming occurs throughout the atmosphere (for all three channels) at a rate of 0.6~0.8 K/Decade. Over Antarctica, a cooling area across the Southern Indian and Atlantic Oceans adjacent to the Antarctic continent is found for all three channels. This cooling area and magnitude appears to be getting larger upward from the mid-troposphere to the lower-stratosphere. Over the Southern Pacific Ocean, the $T_2$ trend is neutral, but a large warming trend (0.3~0.4 K/Decade) is found in the tropopause and lower-stratosphere. Of particular interest, a relatively larger warming over the tip of the Antarctic Peninsula is found for the mid-troposphere. This warming is isolated from the surrounding cooling area over the Southern Atlantic Ocean. It is well known that in situ observations show that the Antarctic Peninsula is warming faster than the rest of the surrounding areas, resulting in significant ice sheet melting in this area. Here the MSU observation is not only consistent with the in situ observations at this particular point, but also provides a more complete trend picture on the entire Southern oceans.

A website has been created for the public to freely acquire the SNO calibrated MSU datasets. The website is under the main page of NESDIS/Center for Satellite Applications and Research and its URL address is http://www.orbit.nesdis.noaa.gov/smcd/emb/mscat/mscatmain.htm. The website contains both the level-1c radiance and level 3 gridded deep-layer temperature datasets. These datasets cover the period from January 1987 to September 2006 that includes observations from NOAA 10, 11, 12, and 14. The radiance datasets with both the SNO calibration and NOAA operational calibration are available. Gridded datasets include 5-day and monthly averages with spatial resolution of $2.5^0$ latitudes by $2.5^0$ longitudes. The monthly data include merged $T_2$, $T_3$, and $T_4$ time series and their anomalies. The pentad data include time series of the merged and individual satellite for these

variables. All the gridded data files are in ASCII text format and reading programs are provided on the website. All these datasets can be downloaded directly from the website.

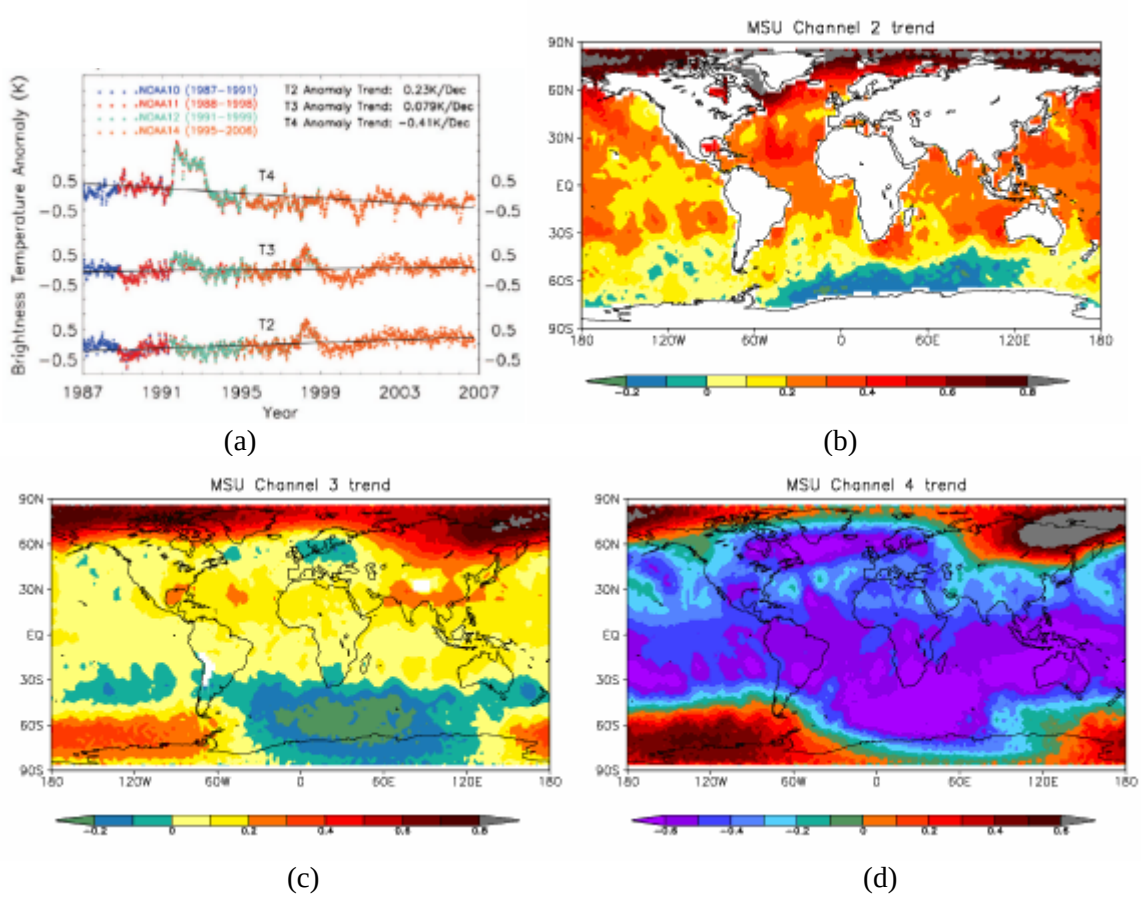


**Figure 16 (a):** Time series and trend observed by the MSU instrument on board NOAA satellites for different atmospheric layers. The abbreviations T2, T3, and T4 refer respectively to temperatures of channels 2, 3, and 4. They represent deep layer temperatures of the mid-troposphere, tropopause, and Lower Stratosphere, respectively.

**(b)**: Spatial distribution of the mid-tropospheric temperature trend for 1987-2006; **(c)** Tropopause temperature trend pattern for 1987-2006; **(d)** Spatial distribution of the lower-stratospheric temperature trend for 1987-2006. Unit in K per decade.

Please visit: http://www.orbit.nesdis.noaa.gov/smcd/emb/mscat/mscatmain.htm